International Journal of Nanomedicine

Dovepress
open access to scientific and medical research

Open Access Full Text Article

ORIGINAL RESEARCH

# Synthesis of meso-tetra-(4-sulfonatophenyl) porphyrin ($TPPS_4$) – CuInS/ZnS quantum dots conjugate as an improved photosensitizer

This article was published in the following Dove Press journal:
*International Journal of Nanomedicine*

Ncediwe Tsolekile[1–3]
Vuyelwa Ncapayi[1,2]
Gabriel K Obiyenwa[2,4]
Mangaka Matoetoe[3]
Sandile Songca[5]
Oluwatobi S Oluwafemi[1,2]

[1]Department of Chemical Sciences (formerly Applied Chemistry), University of Johannesburg, Johannesburg 2028, South Africa; [2]Centre for Nanomaterials Science Research, University of Johannesburg, Johannesburg 2028, South Africa; [3]Department of Chemistry, Cape Peninsula University of Technology, Cape Town 2000, South Africa; [4]Department of Chemistry, Federal University Lokoja, Lokoja, Nigeria; [5]Department of Chemistry, University of Zululand, Kwadlangezwa 3886, South Africa

**Background:** Metal-free, water-soluble and highly stable meso-tetra-(4-sulfonatophenyl) porphyrin ($TPPS_4$) has been studied for their singlet oxygen quantum yield. However, $TPPS_4$ suffers from inherent shortcomings. To address these, $TPPS_4$ was conjugated to ternary copper indium sulphide/ zinc sulphide ($CuInS_2$/ZnS) quantum dots (QDs).

**Purpose:** We herein report for the first time the synthesis of $TPPS_4$–CuInS/ZnS QDs conjugate as an improved photosensitizer.

**Methods:** Water-soluble $TPPS_4$ was synthesized from tetraphenylporphyrin ($TPPH_2$) after silica-gel purification. The CuInS/ZnS QDs were synthesized by hydrothermal method at a Cu:In ratio of 1:4. The porphyrin–QDs conjugate was formed via the daggling sulfonyl bond of the porphyrin and amine bond of the QDs. The effect of pH on the optical properties of $TPPS_4$ was evaluated. The effect of Zn:Cu + In ratio on the ZnS shell passivation was examined to reduce structural defects on the as-synthesized QDs.

**Results:** Various spectroscopic techniques were used to confirm the successful conversion of the organic $TPPH_2$ to water-soluble $TPPS_4$. The singlet oxygen generation evaluation shows an improved singlet oxygen quantum yield from 0.19 for the porphyrin ($TPPS_4$) alone to 0.69 after conjugation (CuInS/ZnS-$TPPS_4$) with an increase in the reaction rate constant (k (s-1)).

**Keywords:** CuInS/ZnS, meso-tetra-(4-sulfonatophenyl) porphyrin, $TTPS_4$, singlet oxygen, conjugation, quantum dots

## Introduction

Singlet oxygen generation and detection has gained much interest within the cancer research field due to its cytotoxic nature and subsequent role in the eradication of cancer/tumor cells.[1] Amongst the many applications of this gaseous inorganic molecule such as the photo-oxidation of toxic molecules and photo-production of chemical intermediates, photodynamic therapy (PDT) still appeals as the most prominent application.[2,3] Several preparative chemical procedures have been reported for the generation of singlet oxygen; eg, thermolysis of 3,3,4,4-tetramethyl-1,2-dioxetane[4] and photosynthesis via plant production.[5] However, photochemical methods, whereby oxygen is irradiated by organic dyes and sensitizers viz. methylene blue and porphyrins, have been shown to produce higher quantities of the molecule.[1] Porphyrins are macro-cyclic molecules that are constituted by four pyrrole subunits that are interconnected by methylene bridge. They are highly conjugated systems with excellent photoelectric and spectroscopic properties.[3]

Correspondence: Oluwatobi S Oluwafemi
Department of Chemical Sciences (formerly Applied Chemistry), University of Johannesburg, PO BOX 17011, Doornfontein 2028, Johannesburg, South Africa
Tel +27 11 559 9060
Fax +27 11 559 6425
Email oluwafemi.oluwatobi@gmail.com

submit your manuscript | www.dovepress.com
DovePress
http://doi.org/10.2147/IJN.S211959

Their inherent ability to generate singlet oxygen upon irradiation with light of specific wavelength and low dark cytotoxicity has resulted in their application in cancer treatment modalities such as PDT.[6,7] In PDT, porphyrins are able to generate singlet oxygen via energy transfer in the excited triplet state to the ground state (triplet) oxygen. Their singlet oxygen efficacy, however, can be affected by environmental factors such as solvent, temperature, moiety attachments and the presence and proximity of quenching groups. Metal-free, water-soluble and highly stable porphyrins such as meso-tetra-(4-sulfonatophenyl) porphyrin ($TPPS_4$) have been studied for their singlet oxygen quantum yield (SOQY), tumor tissue affinity, retention times and water solubility.[8–10] Clinical studies on $TPPS_4$ have shown its potential as a PDT photosensitizer; however, its biological progression has been hampered by the atypical reliance of its photo-physical properties on environmental factors as listed above.

In addressing these inherent shortcomings of $TPPS_4$ and porphyrins at large, much research has focused on conjugated systems for their biological applications.[8,9,11] Moreover, conjugation of $TPPS_4$ has shown to improve the QY of QDs and disaggregation of aged QDs which allows for a wider application range of $TPPS_4$–nanomaterial conjugates.[9] However, binary quantum dots (QDs) adopted to conjugate with porphyrins have added much distress due to their toxic nature attributed to the presence of heavy metals such as Cd and Pb.[12] Consequently, researchers have focused on the use of ternary QDs such as $CuInS_2$/ZnS and $AgInS_2$/ZnS QDs for biological applications. The distinctive optical properties of CuInS-based QDs have resulted in its application in a number of industries and applications such as photovoltaic cells, white light-emitting diodes, bio-medical labeling and imaging.[13,14] Due to the excellent optical properties of these ternary QDs, the conjugation of $TPPS_4$ to these QDs will allow the use of $TPPS_4$ at excitation wavelengths wherein $TPPS_4$ alone cannot be used. Moreover, the conjugation of QDs to $TPPS_4$ is expected to produce a conjugate system with the optical advantages of the QDs while maintaining the treatment efficacy of $TPPS_4$ thereby addressing the inherent challenges of QDs and porphyrins when applied alone in cancer treatment. In this study, glutathione (GSH)-capped CuInS/ZnS QDs were conventionally synthesized using a hydrothermal one-pot process at Cu:In (1:4). The GSH-capped QDs were conjugated to water-soluble $TPPS_4$ porphyrin via sulfonamide bond formation. The effect of pH, temperature and the ratio of porphyrin:QDs on the optical properties of $TPPS_4$ and conjugation was evaluated. Furthermore, the study evaluated the conjugates ability to generate singlet oxygen in the presence of 1,3-diphenylbenzofuran (DPBF) as a singlet oxygen scavenger under spectro-fluorometer laser light at 535 nm. DPBF was selected as a sensitizer due to its ability to rapidly react with dioxygen only and not with super-oxides or ground state (triplet) molecular oxygen.[15] $TPPS_4$ was able to produce singlet oxygen which increased up to three times upon conjugation with highly fluorescent CuInS/ZnS QDs. The as-synthesized materials were characterized by ultraviolet detection (UV), photoluminescence (PL), dynamic light scattering (DLS), transmission electron microscope (TEM), scanning electron microscope (SEM) and nuclear magnetic resonance ($^1$H NMR).

# Materials and methods

## Chemicals

Copper chloride, indium chloride, sodium citrate, L-glutathione, sodium sulfide, zinc acetate, thiourea, benzaldehyde, propionic acid, pyrrole, sodium bicarbonate, ethanol, hydrochloric acid, dichloromethane, methanol, ethyl acetate, n-hexane, chloroform, acetone, di-sodium hydrogen phosphate buffer, petroleum ether, calcium chloride, sulfuric acid, methylene blue, 1,3-diphenylbenzofuran and dimethyl sulfoxide were purchased from Sigma Aldrich. All chemicals were of analytical grade and used without any purification except pyrrole which was distilled prior to use. Deionized water was used for all the aqueous solution preparation.

## Synthesis of $TPPS_4$–CuInS/ZnS conjugates

The synthesis of CuInS core and CuInS/ZnS core/shell (S1), $TPPH_2$ (S2) and $TPPS_4$ (S3), is extensively reported in the supplementary information. The $TPPS_4$ was conjugated to GSH-capped CuInS/ZnS QDs via sulfonamide bond as shown in Scheme 1. Briefly, 2 mL of $TPPS_4$ (1 mg/10 mL $H_20$) was added to 2 mL of CuInS/ZnS (1 mg/10 mL $H_2O$) and stirred for 1 hr at room temperature. The effect of temperature on the conjugation was evaluated by varying the temperature (29°C and 50°C) at which the conjugation was performed. The effect of QDs:porphyrin ratio on the optical properties was evaluated by adding different aliquots of the QDs to $TPPS_4$ porphyrin to obtain a different ratio of $TPPS_4$/QDs between 1:1 and 1:5.

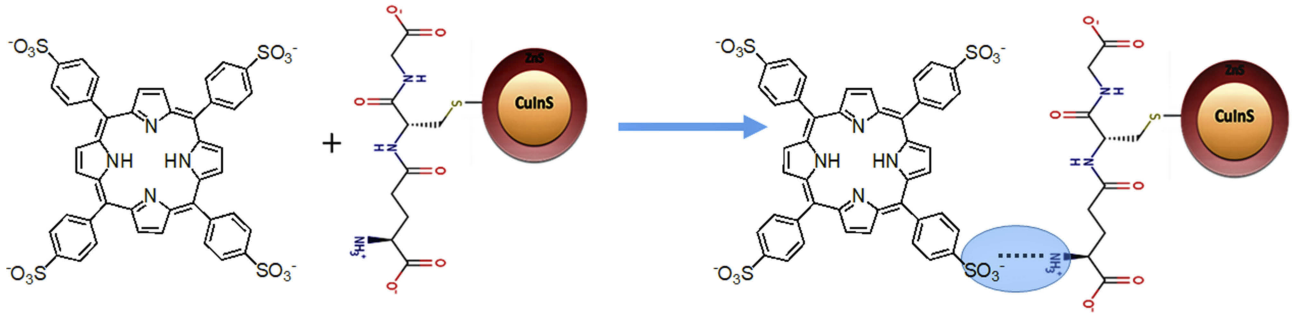


**Scheme 1** Schematic diagram showing the conjugation of CuInS/ZnS and meso-tetra-(4-sulfonatophenyl) porphyrin ($TPPS_4$).

## Singlet oxygen generation of meso-tetra-(4-sulfonatophenyl) porphyrin

Singlet oxygen generation was determined by the Adarsh et al[19] method. Briefly, 1,3-diphenylbenzofuran (DPBF) solution (0.8 mg/25 mL DMSO), methylene blue (MB) solution (0.5 mg/25 mL DMSO), $TPPS_4$ solution (0.20 mg/20 mL DMSO) and CuInS/ZnS–$TPPS_4$ conjugate (1 mg/10 mL) were prepared. Then, 1:1 mixture of DPBF: $TPPS_4$, DPBF:MB, DPBF:$TPPS_4$-CuInS/ZnS conjugate was irradiated at 535 nm (excitation at an absorption wavelength where $TPPS_4$ has minimum absorption and maximum absorption for QDs) using spectro-fluorophotometry laser light for 500 s. The decrease in the intensity of DPBF was monitored at 471 nm. The SOQY was calculated against methylene blue (0.5 mg/25 mL DMSO) as a standard (SOQY =0.52) using the following formula:

$$SOQY = \left(\frac{m_c}{m_{ref}}\right) \times \left(\frac{A_{ref}}{A_c}\right) \times SOQY_{ref'} \quad 1$$

where SOQY and SOQYref are the SOQY of the samples ($TPPS_4$, conjugate) and the reference (methylene blue, 0.52), $m_c$ and $m_{ref}$ are the slope of the samples and reference, $A_c$ and $A_{ref}$ are the absorbance of the samples and the reference at irradiation wavelength.

## Characterization

The synthesized $TPPS_4$, CuInS/ZnS QDs, CuInS/ZnS–$TPPS_4$ conjugate were characterized using Fourier Transform infrared spectroscopy (FTIR) (Spectrum), two UATR spectrometer (Perkin Elmer, UK), photoluminescence (PL) (RF-6000, Shimadzu, Japan), ultraviolet–visible spectrophotometry (UV–vis) (Perkin Elmer UV–Vis Lambda 25 spectrometer, UK), Nuclear Magnetic Radiation (NMR, 500 MHz Bruker spectrometer); Zeta potential analyses were performed using Anton Paar Litesizer 500 (Austria). TEM was done by using JEOL JEM-3010 electron microscope operating at 200 kV.

# Results and discussion

## Structural and optical properties of CuInS and CuInS/ZnS quantum dots

CuInS-based QDs were synthesized hydrothermally (Figure S1) using glutathione as a surface ligand to stabilize the as-synthesized material. Glutathione is tripeptide comprised of three amino acids (cysteine, glycine and glutamic acid), and its backbone structure, therefore, consists of thiol (–SH) group[20] from the cysteine, which was used as a binding group to form GSH-capped CuInS/ZnS QDs. From the glutamic and glycine of GSH, the –COOH and amine groups are available for bonding with other moieties. In this study, FTIR was used to confirm thiol bonding (–SH) on the surface of the CuInS/ZnS QDs. The bands at 3127 $cm^{-1}$ and 1595 $cm^{-1}$ on the GSH spectra represent the N-H and –C=O functional groups, respectively. The shift to 1577 $cm^{-1}$ of the –C=O, the enhancement in peak intensity and broadening of the N–H band, and the disappearance of the –SH peak at 2519 $cm^{-1}$ in the CuInS/ZnS QDs confirm the formation of GSH-capped CuInS/ZnS QDs (Figure 1A).

While the optical properties of QDs lie in the core, the core of QDs is reported to be highly reactive and unstable. Shell passivation with a suitable material is often required in order to improve on these inherent properties while simultaneously improving their photostability.[13] In this study, ZnS was used to form a type 1 band alignment with the CuInS QDs core and thus reduced any lattice mismatch between the core and the shell material. In-situ passivation of the core was performed by injecting $Zn(O_2CCH_3)_2(H_2O)_2$ and $CH_4N_2S$ –

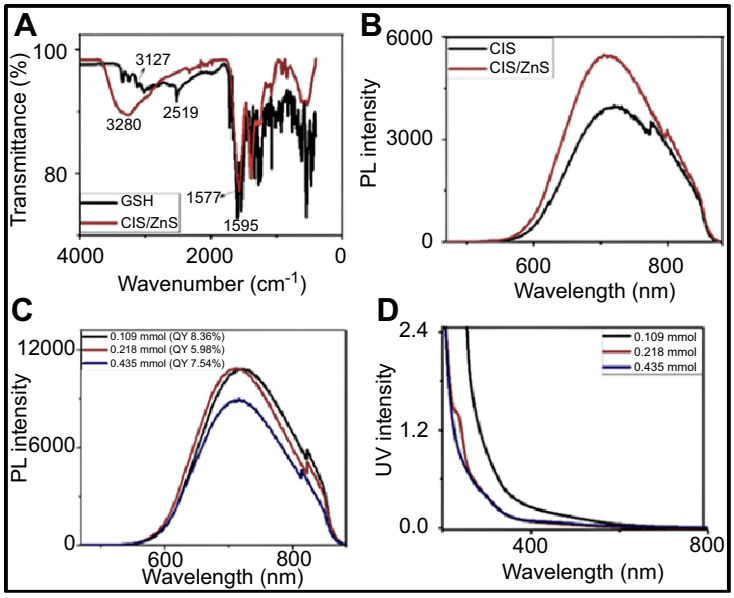


**Figure 1** (**A**) FTIR spectra of GSH and GSH-capped CuInS/ZnS QDs, (**B**) PL spectra of CuInS QDs core and CuInS/ZnS QDs core\shell, (**C**) PL spectra and (**D**) absorption spectra of CuInS\ZnS QDs core-shell at different Zn:Cu + In ratio.

as zinc and sulfur precursors, respectively. Over-coating of the CuInS QDs core with ZnS shell resulted in improved peak intensities and symmetry. The enhancement in the PL intensity is attributed to the effective passivation of the core while the slight blue shifting in the emission position (CuInS QDs em: 721 nm and CuInS/ZnS QDs em: 709 nm) is attributed to the inter-diffusion of the Zn into the core (Figure 1B). The Zn: Cu + In ratio was examined during shell formation in order to minimize the blue-shift observed in the PL spectra of the CuInS/ZnS QDs. Different concentrations of Zn precursor were added during the coating while the Cu:In feeding ratio was kept constant at 1:4. As shown in Figure 1C, a reduction in Zn concentration resulted in a hyper-chromic and red-shifting of the emission peak position (713 nm, 716 nm and 721 nm for Zn at 0.435 mmol, 0.218 mmol and 0.109 mmol, respectively). This red-shifting can be attributed to the reduction of surface defects and stabilization of the QDs structure subsequently leading to radiative recombinations. This is further supported by the improved QY at lower Zn content and thus confirm the reduction in the surface-related recombination trap states after shell passivation. Similar observation has been reported by Zhang et al.[21] Figure 1D shows the absorption spectra of the CuInS/ZnS. A red-shift in the absorption band-edge was obtained with increasing concentration of Zn in the shell suggesting a decreasing trend in the band-gap.

The morphology and average particle size of the as-synthesized CuInS/ZnS corresponding to $[Zn^{2+}]$ =0.200 mmol was estimated from the TEM micrograph (Figure 2A and B). From the TEM, it can be seen that the particles are mono-dispersed and nearly spherical in shape. The average particle sizes of the as-prepared CuInS/ZnS core/shell QDs were estimated to be ~3–3.5 nm. The presence of lattice fringes (Figure 3B) confirmed the crystallinity of the material. Figure 2C and D shows the scanning electron microscope (SEM) of the core/shell, highlighting the selected area that was evaluated for electron dispersive spectroscopy (EDS). The presence of tiny holes on the surface of the CuInS/ZnS QDs was not observed in the CuInS QDS, indicating the difference in surface morphology between the CuInS core and CuInS/ZnS core/shell. The elemental composition of the as-synthesized CuInS core and CuInS/ZnS was characterized using EDS as shown in Figure 2E and F, respectively. From the EDS of the CuInS core (Figure 2E), the elemental composition consisted of Cu, In and S while the EDS of the CuInS/ZnS core/shell (Figure 2F) showed the presence of Cu, In, S and Zn further confirming the formation of the CuInS/ZnS core/shell. The presence of the C was due to the carbon grid used and the O was accounted to the GSH capping.

## Structural and optical properties of meso-tetra-(4-sulfonatophenyl) porphyrin

*meso*-tetra-(4-sulfonatophenyl) porphyrin ($TPPS_4$) was synthesized using *meso*-tetraphenylporphyrin ($TPPH_2$) as

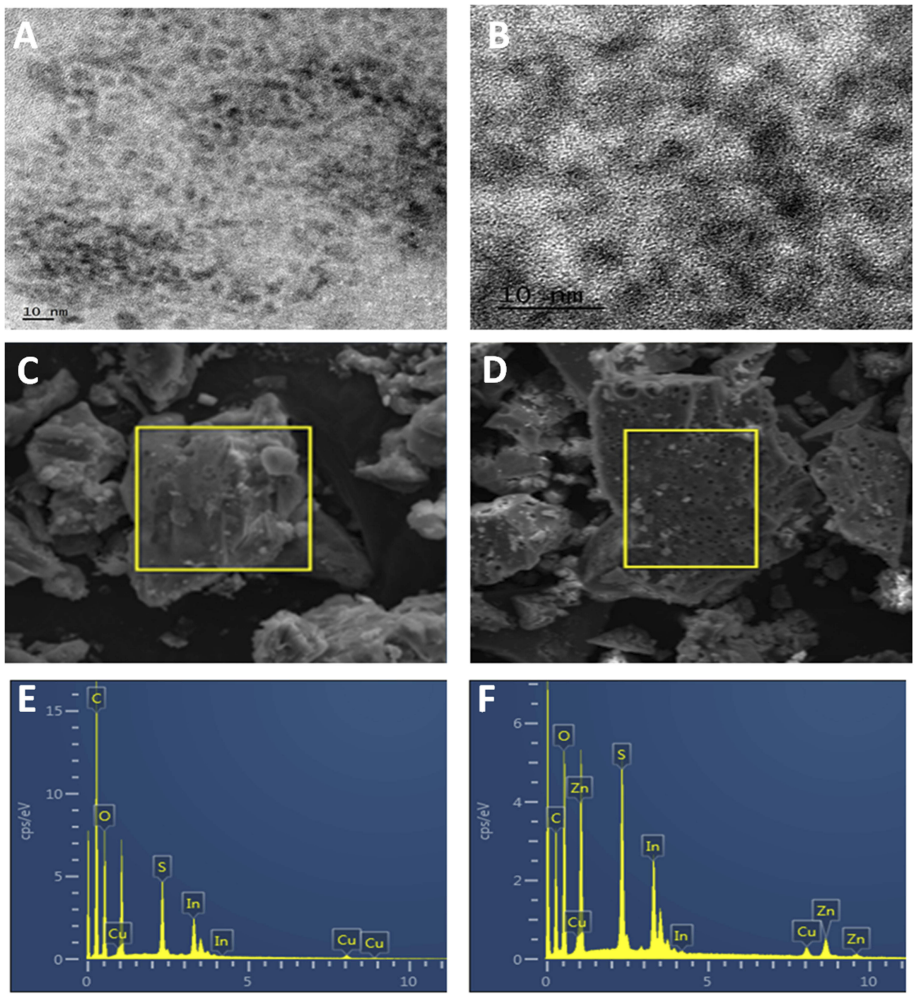


**Figure 2** (**A, B**) TEM images of CuInS/ZnS QDs, SEM of CuInS QDs (**C**) and CuInS/ZnS QDs (**D**) and the EDS of CuInS QDs (**E**) and CuInS/ZnS QDs (**F**).
**Abbreviations:** TEM, transmission electron microscopy; QDs quantum dots ; SEM, scanning electron microscopy; EDS, electron dispersive spectroscopy.

the precursor as seen in S1 and S2. The formation of water-soluble $TPPS_4$ from $TPPH_2$ was confirmed using FTIR, UV and $^1$H-NMR (Figure 3). FTIR spectra (Figure 3A and B) show characteristic peaks of $TPPH_2$ at 3315 $cm^{-1}$, 1474 $cm^{-1}$ and 1443 $cm^{-1}$ assigned to N–H str, –C=C str and C=Nstr of the phenyl, respectively. Upon acidification of the $TPPH_2$, a medium broad peak at 3436 $cm^{-1}$ was formed and assigned to N–$H_{str}$ overlapping with O–$H_{str}$ of absorbed water by the hygroscopic-sulfonated porphyrin. The sharp peak at 1419 $cm^{-1}$ and a medium band at 1595 $cm^{-1}$ are assigned to N–H bend and C–N str frequencies, respectively, which overlapped with C=Cstr of phenyl ring. Sharp bands at 1178, 1118 and 1026 $cm^{-1}$ are attributed to S–O str, confirming the formation of $TPPS_4$.[16,17,22] The changes in the optical absorption spectra from organic precursor $TPPH_2$ to water-soluble $TPPS_4$ are shown in Figure 3C and D, respectively. The changes are characterized by a shift in the UV bands of $TPPH_2$ (Soret: 417 and Q-bands: 514, 549, 589, 647) in comparison to $TPPS_4$ (Soret: 412 and Q-bands: 515, 551, 579, 633). $^1$H-NMR characterization (Figure 3E) of $TPPH_2$ gives chemical shifts at 8.09 and 8.22 (doublet) corresponding to β-pyrrole protons, doublet at 7.58 and 7.72 ppm assigned to the ortho and meta phenyl protons. A decrease in intensity and shielding in the β-protons of $TPPS_4$ are observed at 8.09 ppm and 8.22 compared to $TPPH_2$. The presence of N–H proton signal peaks at −2.66 and −2.39 ppm for the $TPPH_2$ and $TPPS_4$, respectively, and the observed shift in the signals confirm that free base porphyrins ($TPPS_4$) were synthesized from organic $TPPH_2$.

## Effect of pH on $TPPS_4$ optical properties

Spectral changes in the absorption and emission spectra of TPPS4 (in water) at different pH values (pH 8.5 and 3.5;

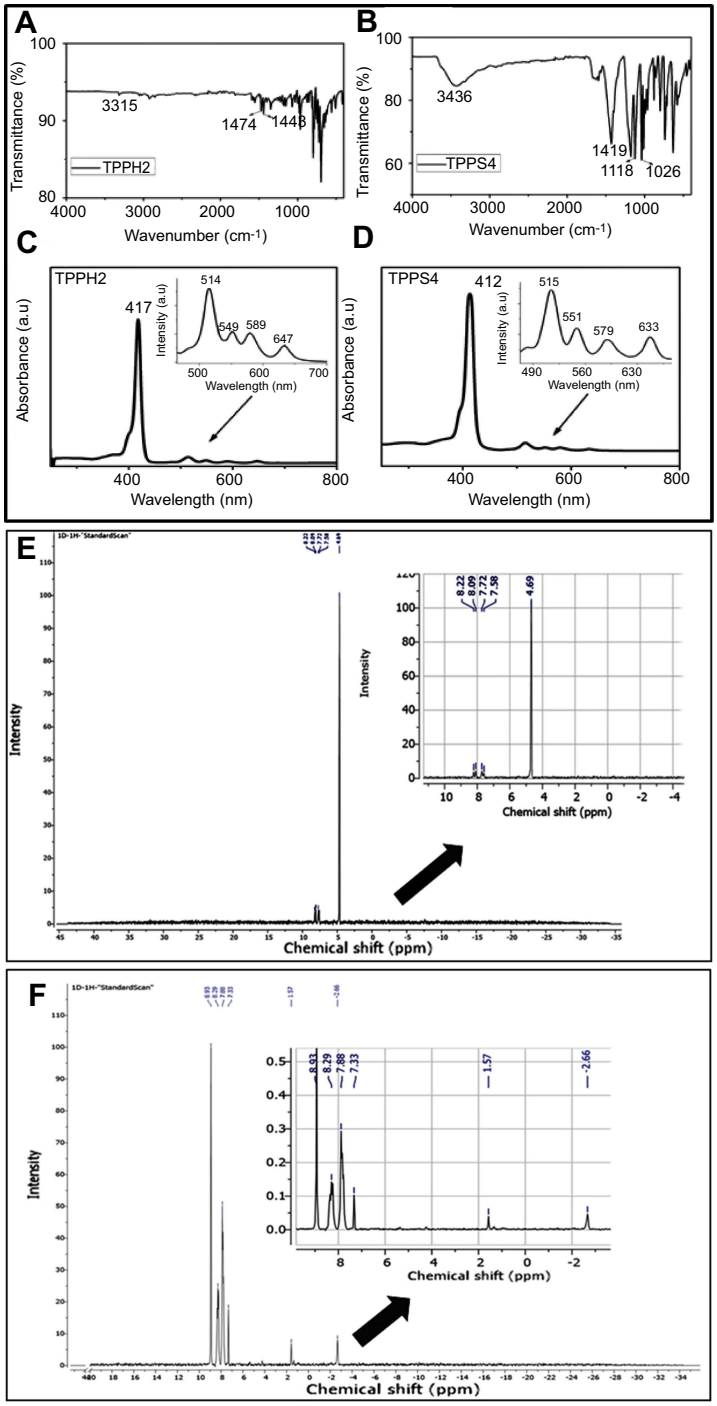


**Figure 3** FTIR spectra of (**A**) $TPPH_2$, (**B**) $TPPS_4$; absorption spectra of (**C**) $TPPH_2$ in DMSO, (**D**) water-soluble $TPPS_4$; $^1H$ NMR spectra of (**E**) $TPPH_2$ and (**F**) $TPPS_4$.
**Abbreviations:** FTIR, Fourier-transform infrared spectroscopy; NMR, nuclear magnetic resonance.

adjusted using phosphate buffer and hydrochloric acid) are shown in Figure 4. In a relatively alkaline medium (pH 8.5), $TPPS_4$ exhibited a typical etio-type porphyrin spectrum (Figure 4A) with Soret band at 412 nm and four Q-bands at 515, 552, 579 and 633 nm. The presence of all four Q-bands suggested that a mono-protonated form of $TPPS_4$ was synthesized in agreement with the $^1H$ NMR. In acidic medium, a red-shift in the Soret bands to 433 nm and the presence of only three Q-bands at 546, 593 and 645 nm was observed. This indicates the formation of one-dimensional ordered arrangements called J-aggregates[23] characteristic of di-protonated $(H^+)_2$ $TPPS_4$ in line with

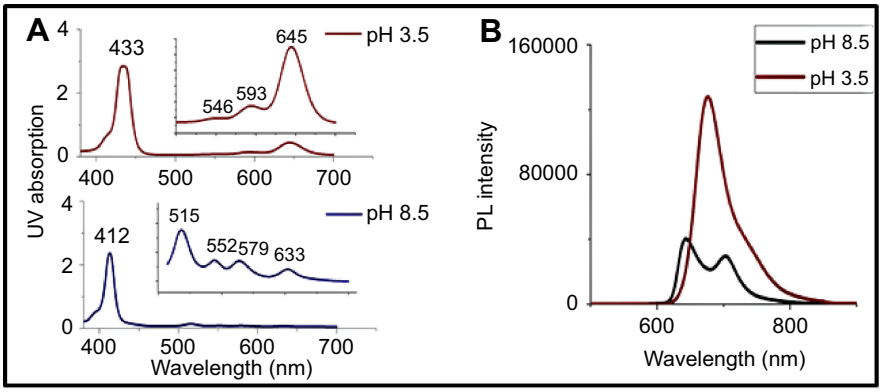


**Figure 4** Effect of pH on (**A**) UV absorption and (**B**) Photoluminescence (PL) emissions of $TPPS_4$.

reported studies.[24] It has been reported that the presence of nitrogen atoms in $TPPS_4$ permits the protonation of the two pyrrolic nitrogens of $TPPS_4$ thereby changing the spectra and energetic properties of the porphyrin. This was observed in the fluorescence studies (Figure 4B) of $TPPS_4$ as a single peak in acidic medium which altered into double peaks in alkaline medium. The two emission peaks at 643 and 703 nm (at pH 8.5) are characteristic of free-base porphyrins in the near-neutral pH region.[25]

In acidic medium, $TPPS_4$ is reported to show decreased quantum yield (QY) triplet state formation and altered electronic absorption spectra with increased Stokes-shifts in the fluorescence spectra[25] as observed in this study (Table 1). Consequently, pH 8.5 was selected for further analysis.

## Effect of excitation wavelength on $TPPS_4$ optical properties

The fluorescence spectra of $TPPS_4$ at different excitation wavelengths is depicted in Figure 5A. Identical emission bands were observed at all the excitation wavelengths with two emission peaks at 643 and 703 nm. The obtained fluorescence results suggested that the emission position of the porphyrin is independent of the excitation energy. The ability of $TPPS_4$ to emit at wavelengths lower than excitation (at scan rate 6000 nm/min) wavelength suggest that it can undergo nonlinear optical processes characteristic of materials with two photon emission property. Maximum emissions were obtained upon excitation at 413 nm, which was consequently selected as the excitation wavelength of $TPPS_4$.

## Conjugation of $TPPS_4$ porphyrin with CuInS/ZnS QDs

To evaluate the binding affinity of the porphyrin on the QDs surface, systematic titration of QDs to porphyrin was performed. The evolution of the emission and absorption spectra of $TPPS_4$ as a function of added CuInS/ZnS QDs is shown in Figure 5B and C. This was performed by keeping the amount of $TPPS_4$ constant in the reaction and increasing the amount of CuInS/ZnS QDs. The PL spectra (Figure 5B) at different QDs concentrations show that with increasing QDs concentration, the optical properties of the conjugate tend toward the QDs; a similar trend is observed in the absorption spectra (Figure 5C). Due to the conjugate instability at increased QDs concentration with changes in optical spectra away from the porphyrin, ratio, 1:1 was selected as optimum ratio for CuInS/ZnS:$TPPS_4$ to maintain the spectroscopic properties of both the porphyrin and QDs within the conjugate.

## Effect of reaction temperature and precursor ratio on the conjugation of CuInS/ZnS–$TPPS_4$

The conjugation reaction was performed at two temperatures (29°C and 50°C) as sulfonamide bond formation is highly dependent on temperature. As previously mentioned,

**Table 1** Effect of pH on the stokes shift of $TPPS_4$

| | Absorption maxima (nm) | Emission maxima (nm) | Stokes shift (nm) |
|---|---|---|---|
| $TPPS_4$ (pH 3.5) | 645 | 677 | 31 |
| $TPPS_4$ (pH 8.5) | 633 | 643 | 9 |

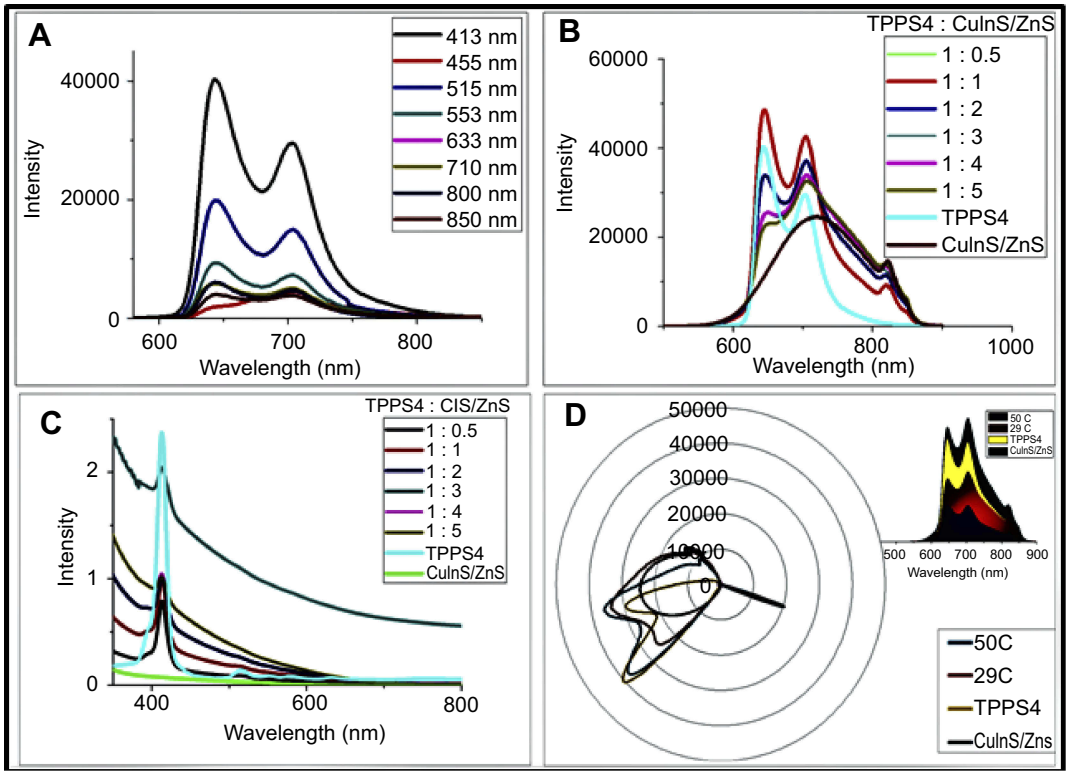


**Figure 5** (**A**) Photoluminescence (PL) spectra of $TPPS_4$ at different excitation wavelengths, (**B**) PL spectra and (**C**) absorption spectra at different CuInS/ZnS:$TPPS_4$ ratios and (**D**) radar chart of CuInS/ZnS–$TPPS_4$ conjugate at different synthetic temperatures (insert: area chart of the conjugate).

the CuInS/ZnS QDs–$TPPS_4$ conjugate maintained the spectral properties of both the porphyrin and QDs; this was observed at both temperatures at which the conjugation was performed. Consequently, a radar chart (Figure 5D) was used to determine the fingerprint of each variable (CuInS/ZnS, $TPPS_4$, CuInS/ZnS-$TPPS_4$) in order to trace the distinct differences in the optical patterns of the as-synthesized material. From the radar chart, we were able to separate the individual optical patterns of each material. The spectra were over-layed in order to specifically distinguish where and how different the conjugates (CuInS/ZnS-$TPPS_4$ at 29°C and 50°C) are from the precursors (CuInS/ZnS and $TPPS_4$). At 29°C, the conjugate fully encompassed the spectral properties of the QDs (as it completely covered the shape of the QDs) while maintaining the spectral shape of porphyrin. However, at 50°C, the conjugate inclined toward the $TPPS_4$ porphyrin (yellow and blue fingerprint) while shifting away from the QDs spectra. This suggests that at reduced temperature, the conjugate formed encompasses both the QD and porphyrin at a greater capacity than at 50°C. Furthermore, from the insert (Figure 5D), the stacked curves show the relative contribution of the QDs and porphyrin to the conjugate. This further confirms that at 29°C, more of the conjugate is likely to be formed as it covers more area than at 50°C. Thus, the synthesis of the conjugate was performed at 29°C.

The electro-kinetic potential of $TPPS_4$ and CuInS/ZnS QDs were measured and found to be −36.4 mV and −74.8 mV, respectively. The negative charge on $TPPS_4$ is attributed to the sulfonate phenyl groups in its structure[11,26,27] while the net negative charge on the surface of the QDs suggests some degree of deprotonation on its surface. This implies a low probable electrostatic attraction between QDs-GSH groups and $TPPS_4$ molecules. However, $TPPS_4$ has four sulfonyl groups available for binding and CuInS/ZnS has amine groups which when combined (sulfonyl and amine group) would aid the formation of sulfonamide bond between $TPPS_4$ and CuInS/ZnS via the negatively charged oxygen of the sulfonate and positive charge of the amine on the GSH-capped QDs (S1). Furthermore, the high affinity of the porphyrin π-conjugated systems for metal surfaces[9] could further foster the formation of the sulfonamide bond. To further confirm the conjugate formation, FTIR analysis was done on the purified and dried CuInS/ZnS QDs, $TPPS_4$ and the dried $TPPS_4$–CuInS/ZnS conjugate. A shift from the CuInS/ZnS QDs and $TPPS_4$ characteristic bands is seen in the conjugate as the O–H

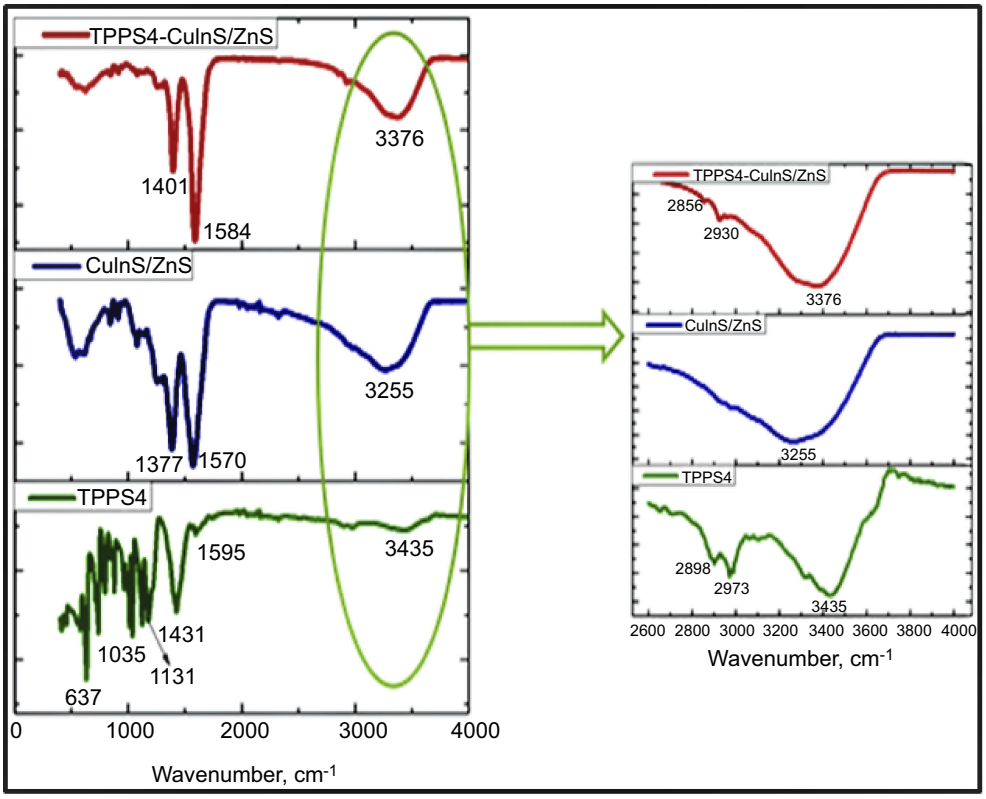


**Figure 6** Fourier-transform infrared spectroscopy (FTIR) of $TPPS_4$, CuInS/ZnS and $TPPS_4$–CuInS/ZnS conjugate.

band shifted to 3376 $cm^{-1}$ from 3435 $cm^{-1}$ of $TPPS_4$. The bands at 1584 $cm^{-1}$ in the conjugate is assigned to –C=O bands observed at 1570 $cm^{-1}$ in the GSH-CuInS/ZnS QDs. Furthermore, the presence of the S=O str at 1401 $cm^{-1}$ band in the conjugate (absent in the CuInS/ZnS QDs spectrum) further confirm the formation of the conjugate (Figure 6).

## Singlet oxygen generation

In this study, singlet oxygen ($^1O_2$) detection was determined via photochemical method using DPBF as a $^1O_2$ trapping agent and methylene blue as a reference. DPBF was chosen as singlet oxygen acceptor because of its ability to rapidly react with $^1O_2$ chemically. Figure 7 represents the kinetics of the singlet oxygen generation as a function of illumination time versus intensity relative to the decay rate of DPBF (at 421 nm) upon scavenging the singlet oxygen generated. The reaction rate constants (k (s-1)) were found to be −0.825±0.068 and −0.69±0.08 for $TPPS_4$ and CuInS/ZnS-$TPPS_4$ conjugate, respectively, as estimated from the slope of regression curve of Figure 7A-B. This indicates that the reaction of the conjugate in the presence of DPBF is much faster than that of $TPPS_4$, implying that the singlet oxygen is generated more rapidly by the CuInS/ZnS–$TPPS_4$ conjugate compared to $TPPS_4$ porphyrin alone. Compared to the synthesized material, the blank (DPBF) reaction rate was constant (Figure 7C) over the measurement intensity range suggesting a higher stability in solution. The kinetic process of the $^1O_2$ generation in the presence of DPBF was presumed to be via the reaction shown below:[1,28–30]

$$TPPS_4 + hv \, {}^1TPPS_4* \longrightarrow 1TPPS_4* \text{ Photo} - \text{activation}$$

$${}^1TPPS_4 \xrightarrow{k_{is}} 3TPPS_4* \text{ Inter} - \text{system crossing}$$

$${}^3TPPS4* + O_2 \xrightarrow{k_\Delta} TPPS_4 + {}^1O_2 \text{ Energy transfer}$$

$${}^1O_2 + DPBF \xrightarrow{k_c} DPBFO_2 \text{ Chemical quenching}$$

From Equation 1, the singlet oxygen generation of the material was calculated. $TPPS_4$ singlet oxygen was measured to be 0.19 which increased to 0.69 upon conjugation with CuInS/ZnS QDs, which is in agreement with the reaction rate constant of the conjugate. The significant increase in the singlet oxygen generation is attributed to the spectral overlap (Scheme S1) of the $TPPS_4$ absorption with fluorescent emission of the CuInS/ZnS as a donor thereby

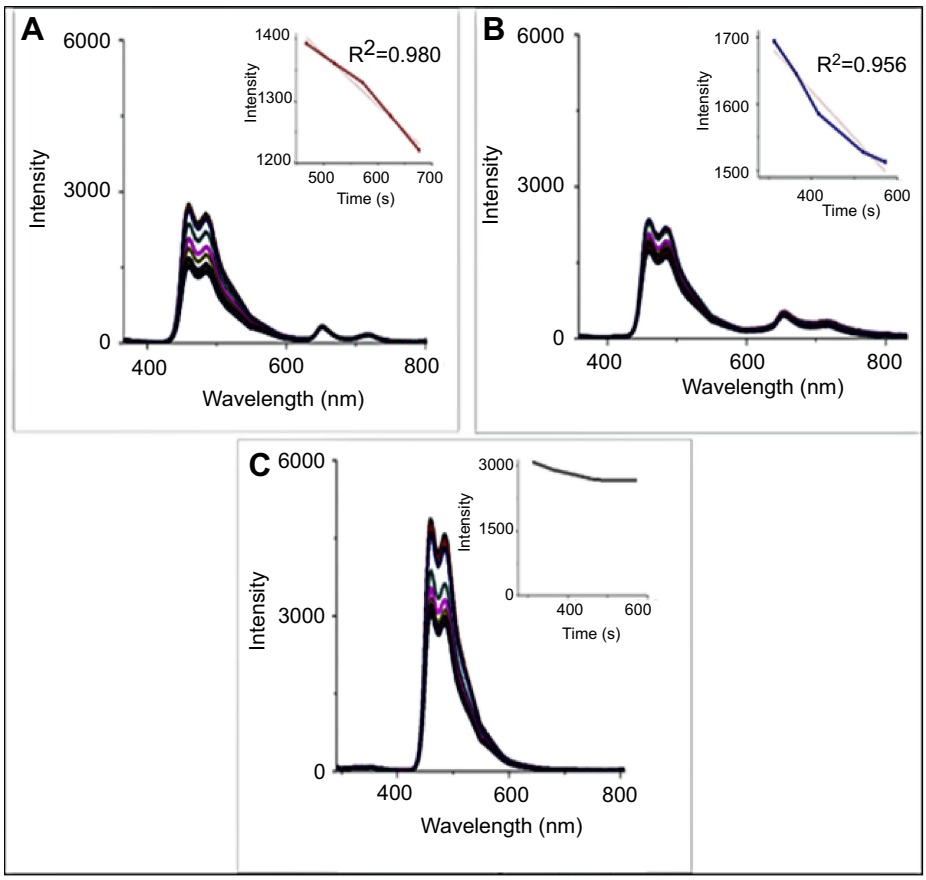


**Figure 7** Singlet oxygen detection of (**A**) $TPPS_4$, (B) CuInS/ZnS–$TPPS_4$ conjugate and (**C**) 1,3-diphenylbenzofuran (DPBF) alone (inserts: changes in emission spectra of DPBF in presence of (**A**) $TPPS_4$, (**B**) conjugate and (**C**) DPBF alone).

suggesting possibility of Forster Resonance Energy Transfer (FRET) between CuInS/ZnS QDs and $TPPS_4$.

## Conclusion

In this study, we successfully synthesized meso-tetra-(4-sulfonatophenyl) porphyrin ($TPPS_4$)–CuInS/ZnS QDs conjugate as an improved photosensitizer. The GSH-capped CuInS/ZnS QDs were synthesized at different Zn:Cu + In ratio during shell formation in order to minimize the blue-shift observed in the PL spectra of the CuInS/ZnS. The emission profile of the QDs improved with a hyper-chromic shift in the PL peaks upon Zn passivation. The photosensitizer- $TPPS_4$ was synthesized using organically soluble $TPPH_2$ as a precursor. The as-synthesized $TPPS_4$ gave characteristic UV absorption spectra in alkaline medium (pH 8.5) whereas at acidic medium (pH 3.5), three Q-bands were obtained consequently, pH 8.5 was used. CuInS/ZnS–$TPPS_4$ conjugate was formed via sulfonamide bond and the ratio of QDs:porphyrin in the conjugate was optimized by varying the amount of QDs in the conjugate. Based on UV, PL and radar chart, a ratio of 1:1 (QDs: porphyrin) was found to be the optimal for the conjugate formation. The effect of temperature on the synthesis of the conjugate showed that optimum temperature for the conjugate synthesis is 29°C. Furthermore, conjugation of the synthesized GSH-CuInS/ZnS to water-soluble $TPPS_4$ porphyrin proved to enhance the singlet oxygen generation of the porphyrin as the SOQY increased from 0.19 for $TPPS_4$ alone to 0.69 upon conjugation. This was supported by the increase in the reaction rate constant of the conjugate compared to $TPPS_4$ porphyrin alone. Thus, the as-synthesized meso-tetra-(4-sulfonatophenyl) porphyrin ($TPPS_4$)–CuInS/ZnS QDs conjugate can be used as an improved photosensitizer in many bio-applications.

## Acknowledgment

The authors would like to thank the National Research Foundation (NRF), South Africa under the Competitive Programme for Rated Researchers (Grant no: 106060), Thuthuka (Grant no: 107295), equipment-related travel and training (Grant no 109892), Cape Peninsula University of Technology and the University of

Johannesburg, South Africa, Faculty of Science Research Committee, and University research Committee, South Africa for financial support. OSO is also grateful to Tohoku University for the two month research visit under the Tohoku University Special Measure.

## Disclosure

Ms Vuyelwa Ncapayi reports grants from National Research Council, during the conduct of the study. The authors report no other conflicts of interest in this work.

## References


1. De Rosa MC, Crutchley RJ. Photosensitized singlet oxygen and its applications. *Coord Chem Rev*. 2002;233–234:351–371. doi:10.1016/S0010-8545(02)00034-6
2. Jeong H, Choi M. Design and properties of porphyrin-based singlet oxygen generator. *Isreal J Chem*. 2015;56:110–1108. doi:10.1002/ijch.201500026
3. Huang H, Song W, Rieffel J, Lovell JF. Emerging applications of porphyrins in photomedicine. *Front Phys*. 2015;3:23. doi:10.3389/fphy.2015.00023
4. Mano CM, Prado FM, Massari J, et al. Excited singlet molecular $O_2$ ($^1\Delta g$) generated enzymatically from excited carbonyls in the dark. *Sci Rep*. 2014;4:5938. doi:10.1038/srep05938
5. Liszkay J. Singlet oxygen production in photosynthesis. *Exper Bot*. 2005;56:37–46.
6. Rajora MA, Lou JWH, Zheng G. Advancing porphyrin's biomedical utility via supramolecular. *Chem Soc Rev*. 2017;46:6433–6469. doi:10.1039/C7CS00525C
7. Rita Giovannetti, 2012:87-109. The Use of Spectrophotometry UV-Vis for the Study of Porphyrins, Macro To Nano Spectroscopy, Dr. Jamal Uddin (Ed.), ISBN: 978-953-51-0664-7, InTech, Available from: http://www.intechopen.com/books/macro-to-nano-spectroscopy/the-use-of-spectrophotometry-uv-vis-for-thestudy-of-porphyrins. Accessed 20 Dcember, 2017.
8. Varchi G, Benfenati V, Pistone A, et al. Core–shell poly-methyl-methacrylate nanoparticles as effective carriers of electrostatically loaded anionic porphyrin. *J Photochem Photobiol Sci*. 2013;12:760–769. doi:10.1039/c2pp25393c
9. Parra GG, Ferreira LP, Gonçalves PJ, et al. Stimulation of cysteine-coated CdSe/ZnS quantum dot luminescence by meso-Tetrakis (p-sulfonato-phenyl)porphyrin. *Nanoscale Res Lett*. 2018;13:40–48. doi:10.1186/s11671-018-2449-x
10. Mahajan NC, Dige BD, Vanjare AR, et al. Synthesis, photophysical properties and application of new porphyrin derivatives for use in photodynamic therapy and cell imaging. *Fluoresc*. 2018;28:871–882. doi:10.1007/s10895-018-2264-x
11. Borissevitch IE, Parra GG, Zagidullin VE, et al. Cooperative effects in CdSe/ZnS-PEGOH quantum dot luminescence quenching by a water soluble porphyrin. *J Luminesc*. 2013;134:83–87. doi:10.1016/j.jlumin.2012.09.008
12. Ruiz S, Pérez OJ. Generation of singlet oxygen by water-stable CdSe (S) and ZnSe(S) quantum dots. *Appl Mater Today*. 2017;9:161–166. doi:10.1016/j.apmt.2017.06.006
13. Kim Y, Lee Y, Kim Y, et al. Synthesis of efficient near-infrared-emitting CuInS $_2$/ZnS quantum dots by inhibiting cation-exchange for bio application. *RSC Adv*. 2017;7:10675–10682. doi:10.1039/C6RA27045J
14. Tsolekile N, Parani S, Matoetoe MC, Songca SP, Oluwafemi OS. Evolution of ternary I–III–VI QDs: synthesis, characterization and application. *Nano-Struct Nano-Obj*. 2017;12:46–56. doi:10.1016/j.nanoso.2017.08.012
15. Guerri F, Lempe E, Lissi EA, Rodriguez FJ, Trull FR. Water-soluble 1,3-diphenylisobenzofuran derivatives. Synthesis and evaluation as singlet molecular oxygen acceptors for biological systems. *J Photochem Photobiol A*. 1996;93:49–56. doi:10.1016/1010-6030(95)04149-4
16. Busby CA, Dinello RK, Dolphin D. A convenient preparation of meso-Tetra(4-sulfonatopheny)porphyrin. *Cancer J Chem*. 1975;53:1554–1555. doi:10.1139/v75-219
17. Meng GG, James BR, Skov KA, Korbelik M. Porphyrin chemistry pertaining to the design of anti-cancer drugs; part 2, the synthesis and in vitro tests of water-soluble porphyrins containing, in the *meso* positions, the functional groups: 4-methylpyridinium, or 4-sulfonatophenyl, in combination with phenyl, 4-pyridyl, 4-nitrophenyl, or 4-aminophenyl. *Cancer J Chem*. 1994;72:2447–2457.
18. Tsolekile N, Ncapayi V, Parani S, et al. Synthesis of fluorescent CuInS/ZnS quantum dots—porphyrin conjugates for photodynamic therapy. *MRS Commun*. 2018;8:398–403. doi:10.1557/mrc.2018.60
19. Adler AD, Longo FR, Finarelli JD, Goldmacher J, Assour J, Korsakoff L. Simplified synthesis for msso-Tetraphenylporphinl. *J Org Chem*. 1967;32:476. doi:10.1021/jo01288a053
20. Heyrovska R. Precise molecular structures of cysteine, cystine, hydrogen-bonded dicysteine, cysteine dipeptide, glutathione and acetyl cysteine based on additivity of atomic radii. *Nat Preced*. 2011;713:1–17.
21. Zhang B, Wang Y, Yang C, et al. The composition effect on the optical properties of aqueous synthesized Cu–in–S and Zn–cu–in–S quantum dot nanocrystals. *Phys Chem Chem Phys*. 2015;17:25133–25144. doi:10.1039/c5cp03312h
22. Bahramian M, Karimipour G, Ghaedi M, Asfaram A, Azad FN, Bazrafshan AA. Application of response surface methodology for ultrasound-assisted rapid adsorption of meso-tetrakis (4-sulfonatophenyl) porphyrin by copper nanowire-loaded in activated carbon: characterization, equilibrium and kinetic modeling. *J Global NEST*. 2015;17:756–770. doi:10.30955/gnj.001754
23. Kelbauskas L, Bagdonas S, Dietel W, Rotomskis R. Excitation relaxation and structure of $TPPS_4$ J-aggregates. *J Luminesc*. 2003;101:253–262. doi:10.1016/S0022-2313(02)00547-1
24. Valanciunaite J, Žerebcova J, Bagdonas S, Streckyt G. Spectroscopic studies of self-assembled $TPPS_4$ nanostructures in aqueous solutions: the role of serumalbumin and pH. *Lith J Phys*. 2004;44:41–47. doi:10.3952/lithjphys.44105
25. Hanyz I, Wróbel D. The influence of pH on charged porphyrins studied nby fluorescence and photoacoustic spectroscopy. *J Photochem Photobiol Sci*. 2002;1:126–132. doi:10.1039/b108837h
26. Gonçalves PJ, De Boni L, Neto NMB, Rodrigues JJ, Zílio SC, Borissevitch IE. Effect of protonation on the photophysical properties of meso-tetra(sulfonatophenyl) porphyrin. *Chem Phys Lett*. 2005;407:236–241. doi:10.1016/j.cplett.2005.03.100
27. Venkatramaiah N, Ramakrishna B, Venkatesan R, Paz FAA, Tomé PCJ. Facile synthesis of highly stable BF3-induced meso-tetrakis (4-sulfonato phenyl) porphyrin ($TPPS_4$)-J-aggregates: structure, photophysical and electrochemical properties. *New J Chem*. 2013;37:3745–3754. doi:10.1039/c3nj00482a
28. Ouchi A, Aizawa K, Iwasaki Y, et al. Kinetic study of the quenching reaction of singlet oxygen by carotenoids and food extracts in solution. Development of a singlet oxygen absorption capacity (SOAC) assay method. *J Agric Food Chem*. 2010;58:9967–9978. doi:10.1021/jf101947a
29. Kuznetsova NA, Gretsova NS, Yuzhakova OA, Negrimovskii VM, Kaliya O, Luk'yanets EA. ulfonated phthalocyanines: aggregation and singlet oxygen quantum yield in aqueous solutions. *Rus J Gen Chem*. 2001;71:36341. doi:10.1023/A:1012369120376
30. Kimel S, Tromberg BJ, Roberts WG, Berns MW. Singlet oxygen generation of porphyrins, chlorins, and phthalocyanines. *Photochem Photobiol*. 1989;50:175–183. doi:10.1111/php.1989.50.issue-2

# Supplementary materials

## S1: Synthesis of CuInS and CuInS/ZnS quantum dots

CuInS quantum dots were synthesized under reflux based on our previously reported method where we used pressure cooker with slight modifications.[18] Briefly; $CuCl_2$ (0.063 mmol), $InCl_3$ (0.25 mmol), sodium citrate (1.00 mmol) and glutathione (0.149 mmol) were added to 100 mL of distilled water under magnetic stirring. The pH of the solution was adjusted to pH 3.60, after which $Na_2S$ (1.25 mmol) was added under strong magnetic stirring. The solution was refluxed at 95°C for 45 mins followed by in-situ growth of the shell. CuInS/ZnS was synthesized via the addition of zinc acetate and thiourea in-situ. The Zn: (Cu + In) ratio was investigated by varying the amount of Zn precursor (0.435 mmol, 0.218 mmol and 0.109 mmol) added into the solution. The reaction was continued for additional 1 hr 15 mins to produce CuInS/ZnS core-shell QDs.

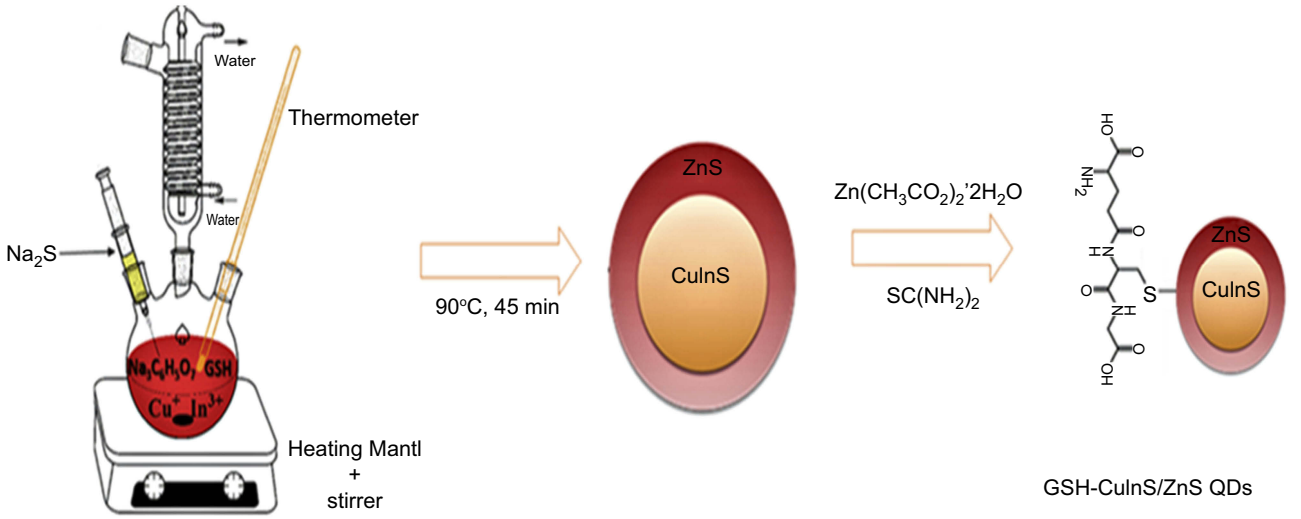


**Figure S1** Hydrothermal synthesis of GSH-capped CuInS/ZnS.

## S2: Synthesis of $TPPH_2$

In a typical reaction, 200 mL of propionic acid was boiled at 141°C. Then, 3.7 mL of freshly purified pyrrole was slowly added in-situ followed by 5.3 mL of benzaldehyde and the solution gradually turned dark brown. The mixture was refluxed for an additional 30 mins after which it was allowed to cool overnight. The obtained purple solution was filtered, and the precipitate was washed with methanol followed by hot distilled water and dried under the fume-hood to obtain 1.0520 g of crude $TPPH_2$.

### Purification of meso-tetraphenylporphyrin ($TPPH_2$)

The crude $TPPH_2$ was purified using a column packed with silica gel (60–70 mesh) as stationary phase and dichloromethane: petroleum ether (3:1) as mobile phase to elute the desired $TPPH_2$.

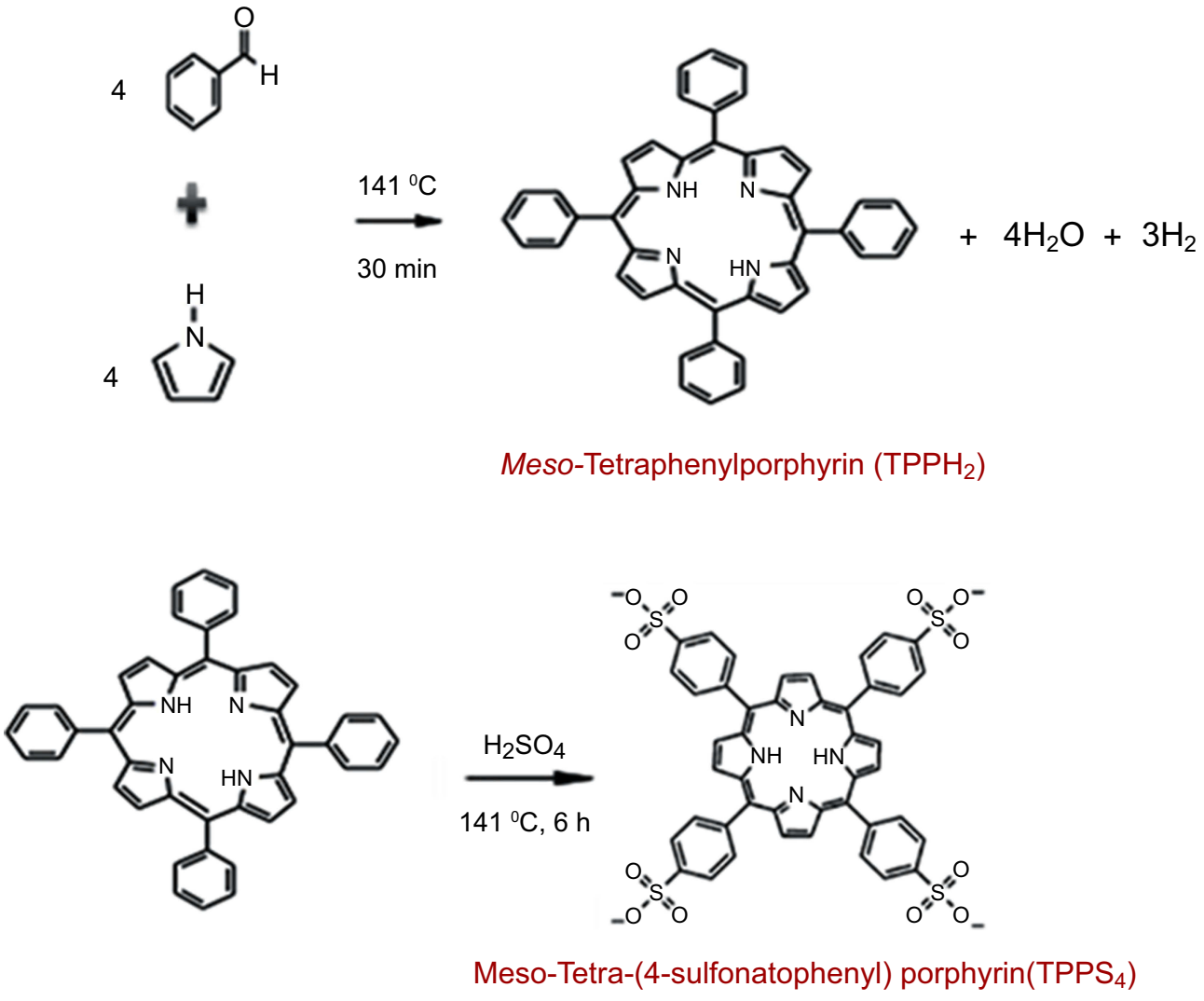


**Scheme S2** Schematic diagram for the synthesis of $TPPS_4$.

## S3: Synthesis of meso-Tetra-(4-sulfonatophenyl) porphyrin ($TPPS_4$)

This was prepared by modifying the reported standard methods.[16,17] In a typical synthetic reaction, concentrated sulfuric acid (10 mL) was added to 0.3952 g of $TPPH_2$ and the solution was heated at 141°C for 6 hrs in a round bottom flask equipped with a drying tube packed with fused calcium chloride. The solution was allowed to cool overnight; then, 75 mL of cold distilled water was added slowly and the resulting green precipitate was washed with 12 mL acetone and allowed to dry. Distilled water (75 mL) was added followed by Celite to further aid the purification of the precipitate. Saturated $NaHCO_3$ was added to neutralize the mixture until the solution turned completely purple while cooling the solution in ice. The solution was filtered to remove the Celite after which the filtrate was concentrated to approximately 45 mL whilst in ice thus precipitating the inorganic salts. The obtained filtrate was washed with methanol, cooled in ice bucket and filtered. The obtained purple residue was washed again with methanol to produce brown solid residue. This was dried overnight in the oven and recrystallized from ethanol/methanol (1:5). The pH of the $TPPS_4$ was adjusted by dissolving the purified $TPPS_4$ in distilled water and adjusting the pH using 0.02 M HCl.